Shortcut Method for Kinetically Controlled Reactive Distillation Systems

J. W. Lee
Dept. of Chemical Engineering, City College of New York, New York, NY 10031

S. Brüggemann and W. Marquardt
Lehrstuhl für Prozesstechnik, RWTH Aachen, D-52056, Germany

A geometric-based shortcut method for reactive distillation is addressed. The rectification body method for nonreactive distillation, the concept of critical Damköhler numbers, and the geometric design method for reactive distillation are combined with a new eigenvector analysis of pinch points. This shortcut method provides a minimum or reasonable Damköhler number for a given heat duty, as well as the design implication of how to effectively distribute reaction zones inside a column. This method can be used for a fast screening of process design alternatives and for an initialization of rigorous optimization.

Introduction

Four important research areas in process design for the 21st Century were introduced: process intensification (Stankiewicz and Moulijn, 2000), process minimization (Hendershot, 2000), process engineering (Keller and Bryan, 2000), and process information (Edgar, 2000). These four articles commonly mentioned reactive distillation as a promising process alternative since initial investment and operating costs are dramatically reduced when compared to processes using single-function equipment. The methyl acetate production system of the Eastman Chemical Company (Agreda and Partin, 1984) is a notable example.

Distillation itself is recognized as an established separation technology in the chemical industry and is well understood with analytical methods, as well as with practical experiences. For reactive distillation, however, there may be few systematic design methods applicable to any type of reaction chemistries even though a lot of articles have been coming out from the 1980s (Taylor and Krishna, 2000; Malone and Doherty, 2000). For example, there is as yet little understanding about how and where to place reaction zones inside a column to maximize the synergistic effect of reaction and separation.

Traditional operation units usually deal with single functionality such as reaction in a reactor and distillation in a column. However, once one superimposes reaction on distillation in one physical shell, it's hard to understand the interaction between V-L phase separation and reaction as the number of components increases. Thus, we would like to propose a shortcut method for reactive distillation to understand this interaction and to analyze reactive distillation systems. This shortcut method will be applied in order to obtain various design insights into reaction distribution in a column, reasonable energy demands, and catalyst holdups with reaction kinetics.

As already pointed out in Okasinski and Doherty (1998), conceptual design and simulation are two different ways in process design, but complementary to each other. When designing reactive distillation columns, required product specs are known in advance. To screen process alternatives in terms of economical attractiveness, it is necessary to know the minimum energy demand and the minimum catalyst holdups. The shortcut approach, as one of conceptual design methods, can quickly estimate these design parameters for the required product specifications, as well as feasibility insights into the combination of reaction and distillation. In contrast to this, simulation repeats calculations by continuously changing these design parameters and necessary inputs (total number of stages, feed stage, number of reactive stages, reaction loca-

Correspondence concerning this article should be addressed to J. W. Lee.

tions, and so on) until we obtain the desired product specs. This is a relatively tedious and time-consuming effort compared to applying a shortcut method. However, if a shortcut method is first used for understanding the process and quickly calculating the critical design parameters, a subsequent simulation or rigorous calculation will be more effective. Thus, shortcut methods greatly facilitate conceptual design.

From the following sections, the rectification body method will be explained (Bausa et al., 1998) for nonreactive distillation and the feasibility will be discussed of a reactive distillation column under reaction equilibrium and with reaction kinetics. The concept of a critical Damköhler number proposed by Buzad and Doherty (1994) will be reviewed and new findings will be emphasized on composition profiles with critical Damköhler numbers. Then, a new mathematical formulation will be proposed to approximate the course of reactive profiles near pinch points without doing rigorous stage-to-stage calculations. Finally, to derive a new shortcut method, rectification bodies will be constructed for nonreactive parts and they will be combined with those with the approximated reactive profile by using eigenvectors of pinch points. Two isomolar and one nonisomolar reactive systems will illustrate the applicability of the shortcut method with a single-feed column.

Rectification Body Method for Nonideal Distillation

Bausa et al. (1998) and Watzdorf et al. (1999) proposed the so-called rectification body method (RBM) to determine the minimum energy demand for a nonreactive azeotropic distillation column. This RBM is applicable to any type of split in nonideal multicomponent mixtures and considers all heat effects in a column. Figure 1 explains the main idea of the RBM. The feedstream (F) containing a mixture of acetone, methanol, and ethanol enters a single-feed distillation column. The top product (D) lies close to the minimum boiling azeotrope between acetone and methanol. The bottom product (B) is pure ethanol.

Rectification bodies are drawn for each rectifying or stripping section by first calculating pinch points using the homotopy continuation method (Seydel and Hlaváček, 1987; Bausa, 2001) and then connecting the pinch points with straight lines. The solid curves inside the rectification bodies in Figure 1 are the possible composition trajectories calculated by using the boundary value method (Levy et al., 1985). The difference among these calculated composition profiles is due to the infinitesimally different fractions of a trace component in the product composition. For example, acetone is a trace component in the bottom product and the composition profiles of the stripping section change greatly according to the fraction of acetone in the bottom product (refer to Figure 1, $x_{B,\text{acetone}} = 10^{-30}$ to 10^{-24}). Thus, the rectification bodies form an approximate envelope for all possible composition profiles.

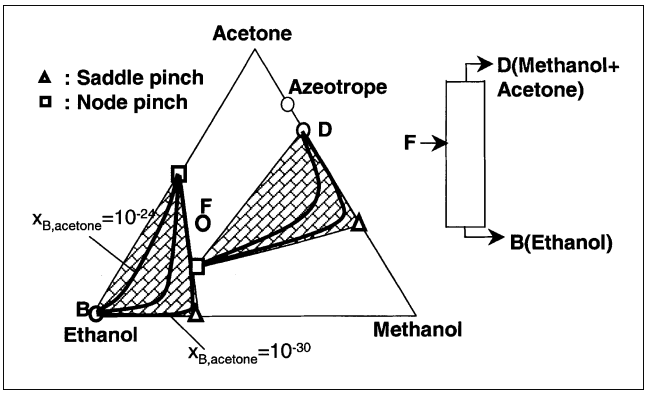

Figure 1. Rectification bodies at a minimum energy demand.

If the two bodies penetrate each other, the specified products are feasible, but the heat is oversupplied. If they do not intersect each other, then we can increase the reboiler (or condenser) duty until the bodies intersect at a single point. The heat duty corresponding to this single point intersection is the minimum energy duty. If such intersection does not occur for any possible heat duty, the product specification is infeasible. Hence, the RBM quickly provides stage profile manifolds and then checks for the intersection in order to determine the feasibility of the specification and calculate a minimum energy demand without rigorous stage calculations.

Reaction Equilibrium vs. Reaction Kinetics

A reactive distillation column with a reactive stripping section can be feasible under reaction equilibrium if the nonreactive rectification body of the rectifying section touches the reactive profile of the stripping section. Reaction equilibrium could reasonably be achieved with a high catalyst holdup or even with a small catalyst holdup for fast reaction. In this case, the reactive composition profile of the stripping section is close to the reaction equilibrium curve. The position of a reactive pinch point for the stripping section is a function of the energy supplied to the separation (Hauan et al., 2000b; Chadda et al., 2000; Lee et al., 2000) along the reaction equilibrium curve. Thus, for a given energy duty, the reactive stripping profile starts from the bottom product composition and ends at the reactive pinch point. Figure 2 shows that, under reaction equilibrium, the minimum energy duty occurs when the reactive profile has a single intersection with the

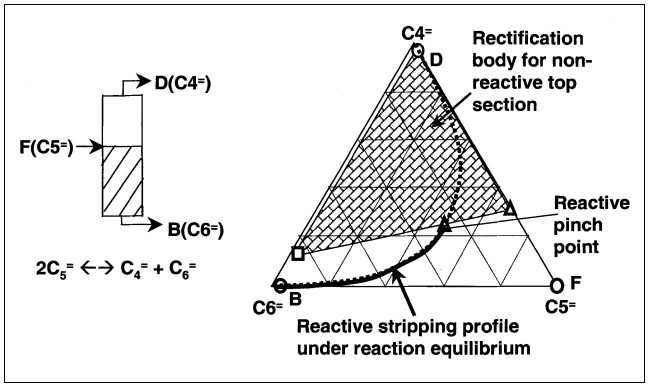

Figure 2. Minimum energy requirement under reaction equilibrium with $2C_5^= \leftrightarrow C_4^= + C_6^=$.

Hereafter, open triangles are for saddle pinches and open squares for node pinches. The dotted curve connecting $C_4^=$ and $C_6^=$ vertices represents reaction equilibrium ($K_{eq} = 0.25$).

nonreactive rectification body. This single intersection ensures the feasibility of this column since reaction equilibrium allows the reaction to proceed until a specified reaction extent is achieved, as in the previous work (Barbosa and Doherty, 1988a,b).

With reaction kinetics, however, the feasibility of a single-feed reactive distillation column requires the intersection between a reactive profile and a nonreactive rectification body for partially distributed reaction zones, while satisfying an overall reaction extent by choosing a proper catalyst holdup. If reaction occurs within both rectifying and stripping sections, the two reactive profiles should intersect and satisfy the overall conversion as in the fixed-point method (Buzad and Doherty, 1994). The reaction conversion is defined by reaction rates on trays that are a function of catalyst volume and a heat duty of either condenser or reboiler (Doherty and Buzad, 1992).

Critical Damköhler number (Da^c)

From this section, the decomposition reaction of 2-pentene into 2-butene and 3-hexene will be used to develop a shortcut procedure. Its kinetics (Okasinski and Doherty, 1998) is summarized in the Appendix. This liquid-phase reaction is assumed to occur only in the stripping section. The critical Damköhler number (Da^c) gives a limiting composition profile for a given heat duty (or a reflux ratio), which passes through a pinch point lying on the reaction equilibrium curve (Buzad and Doherty, 1994). With this critical value, bifurcation occurs at the pinch point in Figure 3. If we slightly decrease the critical Damköhler number, the composition profile travels toward the reverse reaction zone after the pinch point. Epsilon increase in Da^c enables the composition profile to move toward the forward reaction region, and the desired positive reaction conversion can be achieved. One

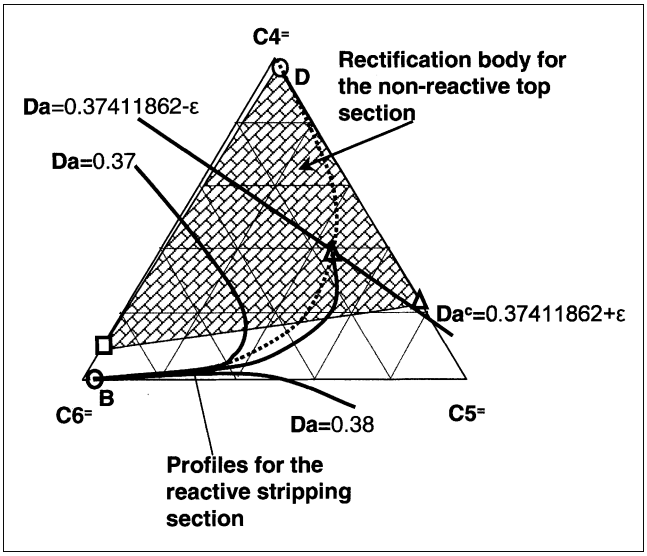

Figure 3. Sensitivity of reactive stage profiles in the stripping section with nearly identical *Da*'s.

$x_F = [0.0, 1.0, 0.0]$, $x_D = [0.98, 0.01992, 0.00008]$ and $x_B = [0.00008, 0.01992, 0.98]$ for $C_4^=$, $C_5^=$ and $C_6^=$. All streams are saturated liquid. External reflux ratio = 2.3.

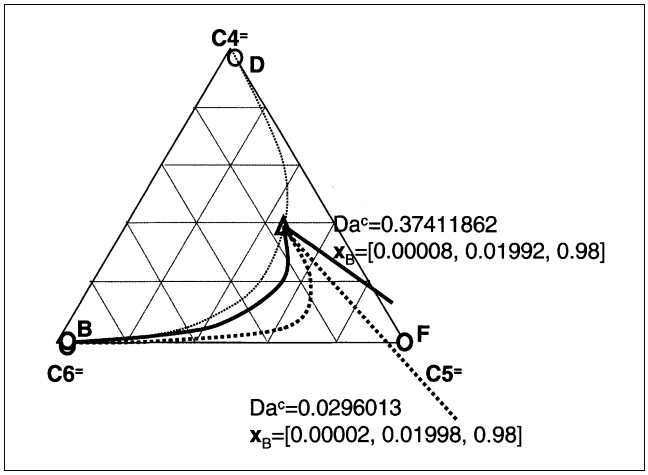

Figure 4. Composition profiles of the reactive stripping section for slightly different bottom product compositions.

should note that the pinch points for reactive sections in a column always lie on the reaction equilibrium curve and their positions are a function of the heat duty of the column (Hauan et al., 2000b; Chadda et al., 2000; Lee et al., 2000). The branches of pinch points for both reactive and nonreactive column sections are obtained using homotopy continuation (Seydel and Hlaváček, 1987; Bausa, 2001). The balance equations for kinetically controlled reactive trays in the stripping or rectifying section are summarized in the Appendix.

The composition profiles are very sensitive to small differences in the Damköhler numbers in Figure 3. For example, the composition profile with $Da = 0.37$ moves into the reverse reaction region, while the composition profile with $Da = 0.38$ partly lies within the forward reaction zone and then moves out of the valid composition simplex. Remarkably, the composition profile with the Da^c is a nearly straight line after the pinch point.

From now on, new findings on the critical composition profile are to be discussed. The critical Damköhler number varies significantly with respect to the amount of trace components in the product compositions, as shown in Figure 4. Taking two bottom product compositions, which differ slightly in the trace component (2-butene ($C4^=$): 0.00008 and 0.00002), we obtain Da^c's of 0.37411862 and 0.0296013. These two Damköhler numbers are different by an order of magnitude. Intuitively, to satisfy a desired reaction extent, the composition profile with the smaller critical Damköhler number should have a larger number of reactive stages, while that with the larger critical Damköhler number should result in fewer reactive stages. Thus, the composition profile of $Da^c = 0.0296013$ has a longer path (dotted curve) than that of $Da^c = 0.37411862$ (solid curve) in Figure 4. Note that the pinch points are almost identical for two slightly different bottom product compositions: [0.3851, 0.4709, 0.1440] and [0.3850, 0.4710, 0.1440] for $C4^=$, $C5^=$ and $C6^=$.

The value of the critical Damköhler numbers is related to the distance between the product composition and the reaction equilibrium curve. As the product composition lies closer to the reaction equilibrium curve, the tray profile starts closer

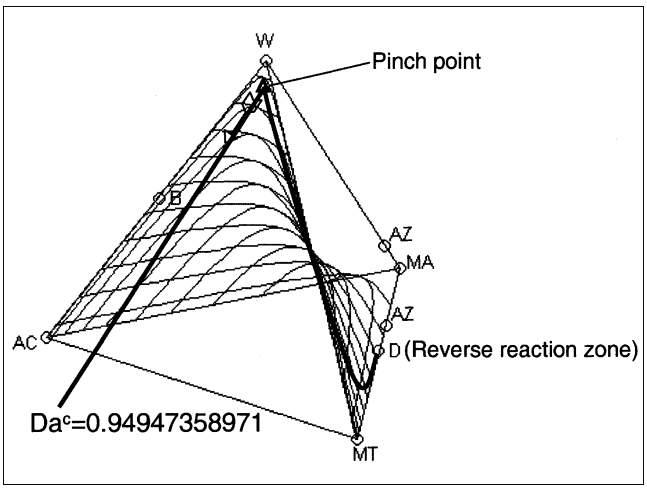

Figure 5. Reactive stage profile of the rectifying section with $Da^c = 0.94947358971$ and the distillate composition in the reverse reaction zone.

x_F = [0.5, 0.5, 0.0, 0.0], x_D = [0.0002, 0.4882, 0.5068, 0.0048] and x_B = [0.49, 0.002, 0.003, 0.505] for AC, MT, MA and W. All streams are saturated liquid. External reflux ratio = 2.0. F/D/B = 2.0/1.0/1.0 kmol/s. The grid surface is the reaction equilibrium manifold at 1 atm. AZ = azeotrope. The arrow is the unstable eigenvector direction of the pinch point (x_P).

to the reaction equilibrium curve and has a shorter course with a larger Da^c. If the product composition is located further away from the reaction equilibrium curve, the tray profile has a longer path with a smaller Da^c, as shown in Figure 4. *Thus, as we put a product composition closer to a reaction equilibrium curve by changing the amount of a trace component, the limiting tray profile has a larger* Da^c. This is an important implication, since it is possible to obtain the limiting composition profiles with Da^c's by manipulating the amount of a trace component in product compositions.

Buzad and Doherty (1994) identified a necessary condition for the existence of this limiting composition profile with $Da = Da^c$: the product compositions should be selected such that the tray profile with $Da = 0.0$ crosses the reaction equilibrium curve. The tray profile with $Da = 0.0$ is a nonreactive profile. So, phase equilibrium determines whether the composition profile with $Da = 0$ will cross the reaction equilibrium manifold. In Figures 3 and 4, the bottom product composition is chosen from the forward reaction zone to satisfy this condition. However, for some reactive systems, it is necessary to select a product composition in the reverse reaction zone due to the behavior of phase equilibrium. For example, the top product composition for the methyl acetate production system must be selected within the reverse reaction zone in order to obtain the limiting composition profile for $Da = Da^c$ as shown in Figure 5. It is confirmed from the stage calculations that the nonreactive profile with $Da = 0.0$ quickly traverses the reaction equilibrium surface from the reverse to the forward reaction zone. Note that even though this mixture is highly nonideal, a straight line satisfactorily approximates the composition profile after the pinch point.

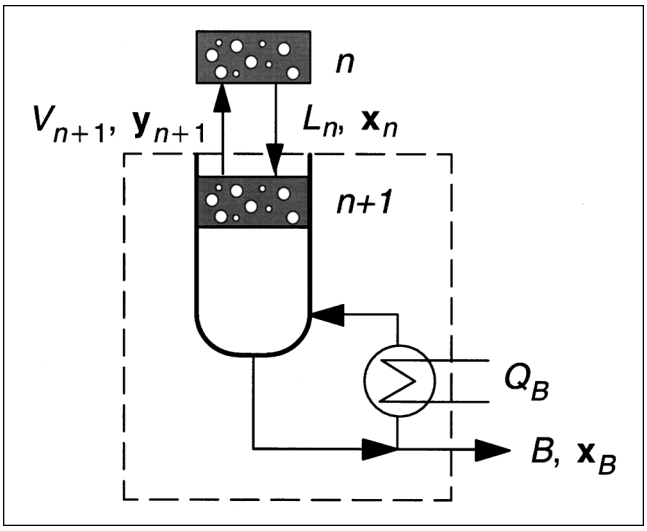

Figure 6. Material balance envelope for the stripping section.

Geometry of Composition Trajectories Close to Pinch Points

Figures 3 to 5 stress the importance of pinch points for determining the global course of the column trajectories. Thus, it is desirable to better understand the behavior of a trajectory in the vicinity of a pinch point. For nonreactive distillation processes, Julka and Doherty (1990) present a method to determine the qualitative behavior of the distillation map close to a pinch point by applying nonlinear dynamic systems theory to the set of tray equations. They concluded that the distillation map represents a tray-by-tray recurrence with (C-1) degrees of freedom. For convenience, the liquid concentrations on each plate are chosen as the free variables, while vapor composition and temperature are implicitly calculated from the phase equilibrium and summation equations. In this case, the liquid concentration on stage n in the stripping section can be calculated from the mass balance around this stage according to the balance system shown in Figure 6

$$x_{n,i} = \frac{V_{n+1}}{L_n} y_{n+1,i}(x_{n+1}, T_{n+1}) + \frac{B}{L_n} x_{B,i}, \quad i = 1...C \quad (1)$$

The formulation for the rectifying section can be chosen analogously. At the pinch, the driving force of the separation vanishes and the map is given by

$$x_i = f_i(x) = \frac{V_P}{L_P} y_i^*(\boldsymbol{x}_P, T_P) + \frac{B}{L_P} x_{B,i}, \quad i = 1...C \quad (2)$$

Applying dynamic systems theory, the local topology of the profiles in the vicinity of a pinch point is defined by the eigenvalues and eigenvectors of the Jacobian of the map evaluated at the pinch point

$$\boldsymbol{J} = \left(\frac{\partial f_i}{\partial x_j} \right), \quad i,j = 1...C \quad (3)$$

Julka and Doherty (1990) point out that $\boldsymbol{J}$ always has (C-1) real, nonzero eigenvalues and a complete set of eigenvectors

for all liquid-phase compositions within the composition space. Let λ_i be the eigenvalues and $\boldsymbol{u}_i$ be the eigenvectors of this matrix. The stability of the eigenvectors is characterized by the respective eigenvalues:

$|\lambda_i| < 1$: Stable eigenvector, that is, the profile is attracted towards the pinch in this direction.

$|\lambda_i| > 1$: Unstable eigenvector, that is, the profile is repelled from the pinch in this direction.

Following this concept, each pinch point can be classified as unstable node, saddle, and stable node. For details, see Julka and Doherty (1990) or Bausa (2001).

In kinetically controlled reactive distillation processes, the extents of reaction $\xi_{r,n}$ are introduced as N_R degrees of freedom of the tray-by-tray recursion in addition to the liquid composition $\boldsymbol{x}_n$. Here, N_R is the number of independent reactions. The conversion on each plate can be described by some formulation of the kinetic behavior of the reactive mixture. However, for the sake of generality, no specific formulation is introduced here. Instead, let $g_r(\boldsymbol{x},T_{n+1})$ describe the reaction rates of each reaction on a plate. Observing the contribution of the reactions in the mass balance, the tray-by-tray recursion is then given by

$$x_{n,i} = \frac{V_{n+1}}{L_n} y_{n+1,i} + \frac{B}{L_n} x_{B,i} - \sum_{r=1}^{N_R} \frac{\xi_{r,n+1}}{L_n} \nu_{r,i}, \qquad i = 1...C$$
$$\xi_{r,n} = g_r(\boldsymbol{x},T_{n+1}) + \xi_{r,n+1}, \qquad r = 1...N_R \tag{4}$$

The mapping at the pinch is, therefore, described by

$$x_i = \frac{V_P}{L_P} y_i^*(\boldsymbol{x}_P,T_P) + \frac{B}{L_P} x_{B,i} + \sum_{r=1}^{N_R} \frac{\xi_{r,P}}{L_P} \nu_{r,i} = f_i(\boldsymbol{x}_P) \qquad i = 1...C$$
$$\xi_{r,P} = g_r(\boldsymbol{x},T_P) + \xi_{r,P}, \qquad r = 1...N_R \tag{5}$$

For a given heat duty, the reactive pinch points will be determined on the reaction equilibrium manifold (Chadda et al., 2000), where $g_r(\boldsymbol{x}_P, T_P)$ in Eq. 5 is equal to zero. If more than one reaction is involved, the reactive pinch points will lie on the intersection of the equilibrium manifolds for each reaction. The reactive pinch points are calculated using a homotopy continuation algorithm. For details on this calculation, refer to Bausa (2001).

Analogously to the nonreactive case, the local topology in the vicinity of the pinch is defined by the eigenvalues and eigenvectors of the Jacobian

$$J = \begin{pmatrix} \dfrac{\partial f_i}{\partial x_j} & \dfrac{\partial f_i}{\partial \xi_l} \\ \dfrac{\partial g_r}{\partial x_j} & \boldsymbol{I}_{N_R} \end{pmatrix}, \quad i,j = 1...C \qquad r,l = 1...N_R \tag{6}$$

where $\boldsymbol{I}_{N_R}$ is the identity matrix of dimension N_R. Note that there are now $(C - 1 + N_R)$ eigenvalues and eigenvectors, that is, each reaction contributes an additional eigensolution. Moreover, the eigenvectors describe the linear approximation of the column profile in the space of liquid-phase concentrations and extents of reaction close to the pinch.

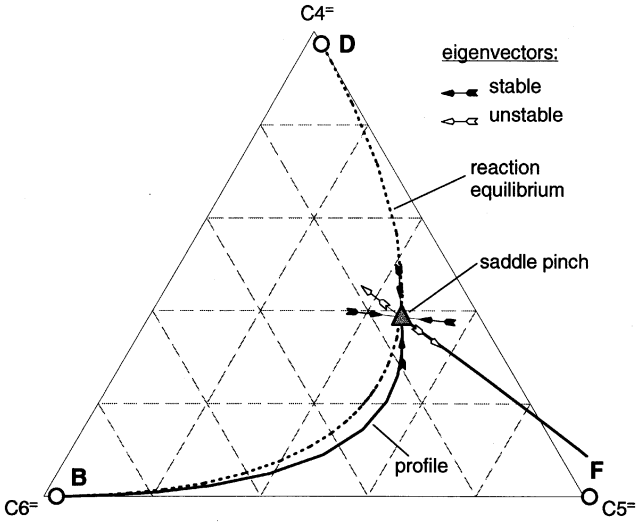

Figure 7. Geometry of the profiles close to the pinch point.

Figure 7 shows the projection of a stripping section column profile and the eigenvectors of the pinch point onto the composition space for the 2-pentene decomposition example discussed above. Here, a bottoms product composition of $\boldsymbol{x}_B = [0.00008, 0.01992, 0.98]$, a reflux ratio of $r = 2.3$, and a dimensionless holdup of $Da = Da^c = 0.37411862$ were chosen. According to the derivation presented above, a total of $(C-1+N_R) = 3$ eigenvalues are obtained (see Table 1). One of these is greater than 1 and, thus, corresponds to an unstable eigenvalue, while the absolute value of the other two are smaller than 1 and, thus, denote the stable eigenvalues. The pinch therefore constitutes a saddle of the distillation map. It can be seen that the calculated profile leaves the pinch in the direction of the eigenvector associated with the unstable eigenvalue. Since the profile does not exhibit significant curvature, it is well described by a linear approximation using this unstable eigenvector. This characteristic behavior of kinetically limited reactive profiles will be exploited in the design method presented in the following sections. Since two stable eigenvectors exist, there is no single direction in which profiles are attracted towards the pinch. As a matter of fact, they can approach the pinch from any linear combination of the two stable eigenvectors. However there is only one single profile originating from the bottom product concentration, and, thus, corresponding to a feasible distillation column.

Table 1. Eigenvalues and Eigenvectors at Pinch Point in Figure 7

Type		Unstable	Stable	Stable
Eigenvalue λ_i		1.5906	−0.2486	0.5457
Eigenvector $\boldsymbol{u}_i$	x_{C4}	0.2568	0.0681	0.7525
	x_{C5}	−0.4174	−0.5538	−0.4025
	x_{C6}	0.1606	0.4857	−0.3500
	ξ	−0.4284	0.3364	0.1932

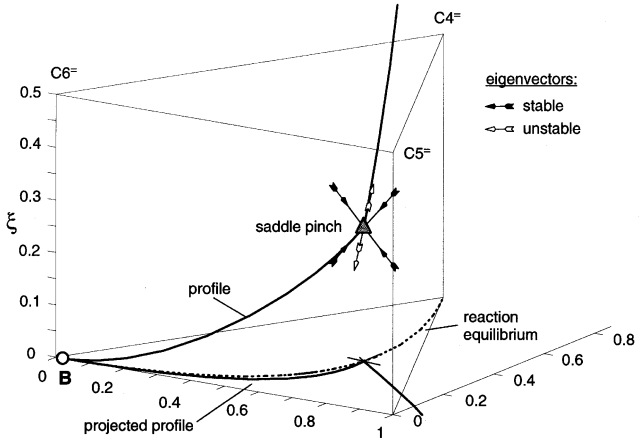

Figure 8. Geometry of reaction extent close to the pinch point.

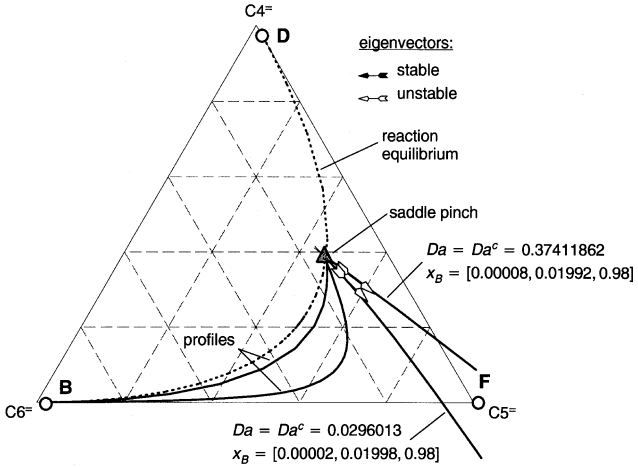

Figure 9. Estimate of the composition profiles after the pinch point by unstable eigenvector directions for two different profiles.

With $Da = Da^c$, this profile approaches the pinch exactly in the direction of one of the stable eigenvectors. Therefore, this profile describes a separatrix of the distillation map for a given bottom product composition.

The three-dimensional (3-D) view in Figure 8 shows the extent of reaction. The representation is identical to Figure 7, however, the additional coordinate axis shows the accumulated extent of reaction (ξ). Here, $\xi = 0$ has been chosen at the starting point of the profile (the bottom product B). Moving along the column from the bottom product towards the feed stage, the accumulated extent of reaction increases. The quality of the approximation of the profiles by their respective unstable eigenvectors is further highlighted by revisiting Figure 4. As already discussed, the profiles shown in this figure are characterized by a strong sensitivity with respect to the trace concentrations of $C_4^=$ in the bottom product. Figure 9 shows the two profiles and the respective eigenvectors. The stable eigenvectors have been omitted for better legibility. The sensitivity of the profiles is captured by the eigenvector directions.

Shortcut Method for Reactive Distillation Based on Eigenvector Directions

In the two previous sections, several important characteristics of the composition profiles with Da^c's are pointed out. The most important one is that these limiting composition profiles in Figures 4 and 5 follow the same pattern; starting from the product composition, they approach the pinch points and continue to proceed into the forward reaction zone. Thus, the path of composition profiles with Da^c's is quite predictable. After the pinch point, they can be approximated by the directions of unstable eigenvectors (see Figure 9). Figure 3 shows that the reactive profile with $Da = Da^c$ is the limiting profile for $Da \geq Da^c$. This limiting profile offers the largest path of interaction with the nonreactive rectification body of the rectifying section. Since such interaction is a necessary condition for the feasibility of the split, this choice of $Da = Da^c$ gives the highest likelihood of finding feasible operating conditions. For $Da > Da^c$, the size of the path of the intersection decreases until no intersection is achieved at all (see profile with $Da = 0.38$ in Figure 3). If $Da < Da^c$, intersection is achieved, however, the overall reaction extent can never be satisfied since those profiles lie within the reverse reaction region.

In summary, the reactive composition profiles with Da^c are used to develop a shortcut method since: (1) their paths are predictable; (2) they can be estimated by the directions of unstable eigenvectors, as in Figures 7 to 9; (3) they lie within the forward reaction zone and, therefore, correspond to profiles with positive conversions; and (4) they are the limiting case for the profile intersection.

As seen in Figure 4, Da^c shows a strong sensitivity to the distance of the product composition from the reaction equilibrium curve, whereas the location of the pinch point is not sensitive to such small perturbations of the product composition. For the conceptual design of the reactive distillation process, such small deviations from the specified product composition will usually be tolerable. Hence, Da^c can be chosen freely as a design degree of freedom if small deviations from the specified product composition are allowed. However, Da is still constrained by the two necessary conditions for feasible separation: (1) Intersection of rectifying and stripping section profiles or rectification bodies; (2) satisfaction of a specified overall extent of reaction.

Figure 10 shows the unstable eigenvector directions of the pinch point with $Da_1 = 0$ and $Da_2 = 1{,}000$. Between these two eigenvector directions, we can determine an estimated composition profile corresponding to $Da_1 \leq Da \leq Da_2$. Here, the maximum $Da = 1{,}000$ is equivalent to $Da \rightarrow \infty$ since the unstable eigenvector direction does not change above $Da =$ 1,000. However, this value changes depending on reactive mixtures and the location of reaction zones, which is easily confirmed by eigenvector calculations with various Da's. Even though a reactive composition profile is not physically available when Da is zero, the unstable eigenvector is mathematically available and its direction is chosen as the composition profile with the minimum Da. Once the liquid composition profile is estimated, the corresponding vapor composition profile is calculated by the phase equilibrium relationship, as in Figure 10.

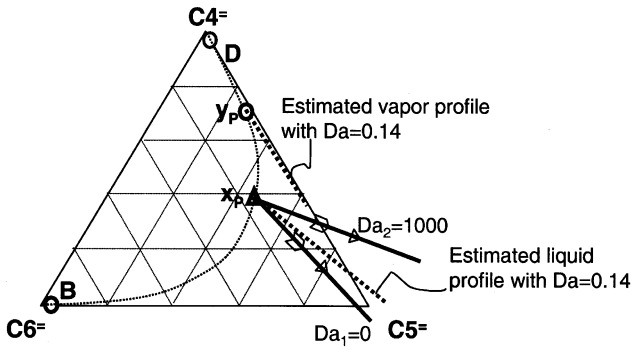

Figure 10. Linear estimation for the liquid and vapor profiles after the pinch point by using unstable eigenvector directions.

The dotted line of the estimated liquid composition profile corresponds to the unstable eigenvector direction with $Da = 0.14$.

Now, we geometrically determine the final liquid composition ($\boldsymbol{x}_{n+1}$) on the estimated liquid composition profile by enforcing the specified overall reaction extent in Figure 11. In composition space, the total cascade difference point (δ_t) represents the overall reaction extent (Lee et al., 2001b). The straight line connecting the bottom product composition and the total cascade difference point is the cascade difference point trajectory, which describes reaction extents on each reactive stage of the stripping section, as in Eq. 7

$$\boldsymbol{\delta}_n = \frac{B\boldsymbol{x}_B - 2\xi_n \boldsymbol{c}_P + 2\xi_n \boldsymbol{c}_R}{B} \tag{7}$$

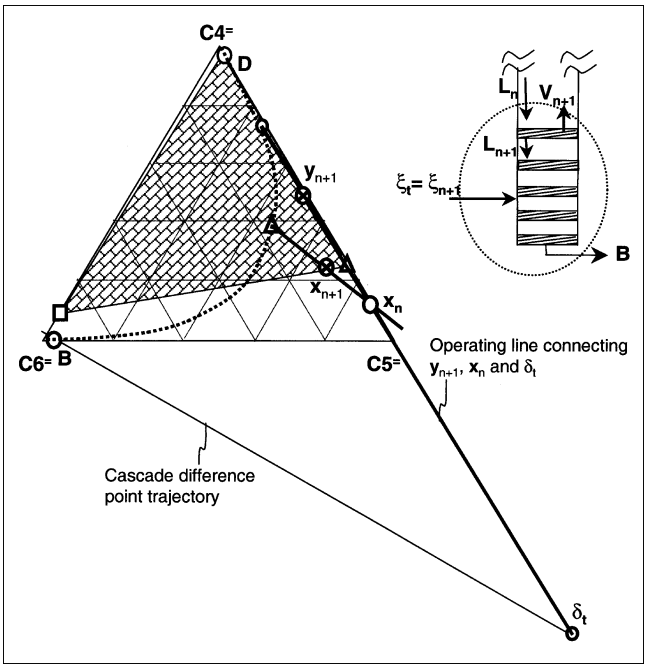

Figure 11. Determination of the vapor and liquid compositions at the final reactive stage (stage $n+1$) of the stripping section.

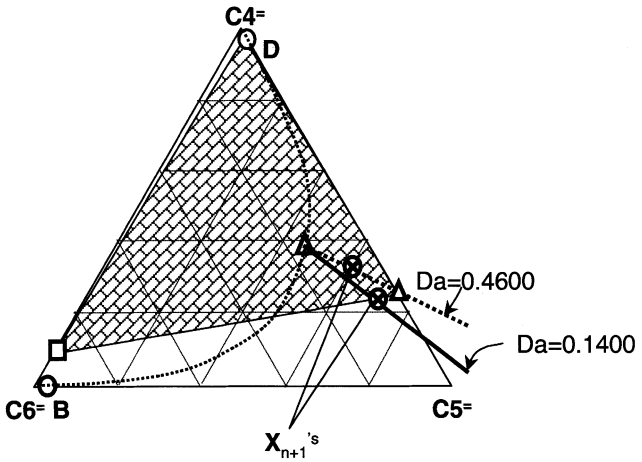

Figure 12. Minimum Damköhler number corresponding to the liquid composition at the final reactive stage having a single intersection with the nonreactive rectification body.

Two solid lines for the estimated profile and the operating line describe the minimum $Da = 0.1400$, while two dotted lines represent $Da = 0.4600$.

where $\boldsymbol{c}_P$ and $\boldsymbol{c}_R$ are the normalized product and reactant coefficient vectors, $\boldsymbol{c}_P = [1/2\ 0\ 1/2]$, and $\boldsymbol{c}_R = [0\ 1\ 0]$ for $C_4^=$, $C_5^=$ and $C_6^=$, respectively. As the reaction extent increases, the cascade difference point (δ_n) at stage n approaches δ_t.

For a given feed and product specification (that is, composition, flow rate, temperature and pressure), the overall reaction conversion should be satisfied at the top reactive stage (stage $n+1$ in Figure 11) of the stripping section if the reaction extent is added up from the bottom to this final stage. In addition to that, the liquid composition at the final reactive stage should intersect the rectification body of the nonreactive rectifying section in order to have a feasible column. Figure 11 shows the corresponding geometrical construction. The material balance around the whole stripping section is

$$L_n\boldsymbol{x}_n = V_{n+1}\boldsymbol{y}_{n+1} + B\boldsymbol{x}_B - \boldsymbol{\nu}\xi_{n+1} = V_{n+1}\boldsymbol{y}_{n+1} + \delta_{n+1}\xi_{n+1} \tag{8}$$

A certain liquid composition ($\boldsymbol{x}_n$) entering down to the balance envelope lies between the straight line connecting the vapor composition at stage $n+1$ ($\boldsymbol{y}_{n+1}$) and the total cascade difference point ($\delta_t = \delta_{n+1}$). Thus, we enforce this overall reaction extent ($\xi_t = \xi_{n+1}$) to be satisfied from the bottom to the final reactive stage ($n+1$) in Figure 11. So, the positions of the liquid composition ($\boldsymbol{x}_n$) and the vapor composition at the final reactive stage ($\boldsymbol{y}_{n+1}$) are simultaneously determined on the estimated liquid and vapor profiles by the heat balance. To ensure the feasibility of this column, the liquid composition at the final reactive stage ($\boldsymbol{x}_{n+1}$), which is determined by the phase equilibrium calculation with $\boldsymbol{y}_{n+1}$, should touch or penetrate the rectification body of the nonreactive rectifying section.

All the procedures explained in Figures 10 and 11 for the reactive stripping section can be used analogously for a reactive rectifying section. Thus, the algorithm for a new shortcut

method for a reactive distillation column with a stripping or rectifying reaction zone is summarized as follows:

(1) Specify a column pressure and give the feed and product specifications. From these specifications, the overall reaction conversion (or δ_l) results.

(2) Set an external reflux or reboil ratio (heat duty).

(3) Obtain a rectification body for the nonreactive section and the pinch points of the reactive section.

(4) Choose *Da*.

(5) Calculate the eigenvectors at the pinch and approximate the reactive liquid and vapor composition profiles.

(6) Determine the liquid and vapor compositions at the final reactive stage on the estimated profiles by construction with the total cascade difference point.

(7) Check for the intersection between the liquid composition at the final reactive stage ($\boldsymbol{x}_{n+1}$ in Figure 11) and the rectification body of the nonreactive section.

(8) If the intersection is not achieved, choose different *Da* and go to step 5. If the intersection cannot be achieved for any choice of *Da*, increase the heat duty and go to step 3.

In step 1, the product compositions of the reactive section should be selected such that the critical composition profiles can exist, as already explained in Figures 4 and 5. The selection of an appropriate $Da > 0$ for approximation of the reactive profiles in steps 4–8 needs several iterations. From our experience, a bisection strategy starting with $Da = 0.01$ and $Da = 10$ leads to the desired Damköhler number quickly.

The minimum Damköhler number for a given heat duty corresponds to the liquid composition at the final reactive stage ($\boldsymbol{x}_{n+1}$) just intersecting the nonreactive rectification body in Figure 12. When the final liquid composition lies inside (or penetrates) the nonreactive rectification body, the Damköhler number increases from the minimum value of 0.1400 to 0.4600. Using the design procedure, we can thus obtain a minimum *Da* for a given heat duty.

The heat duty should be increased if there is no intersection between the final liquid composition and the rectification body even with a very large *Da*, as shown in Figure 13a for $r = 1.5$. If the reflux ratio increases from $r = 1.5$ to $r = 1.67$, the final liquid composition ($\boldsymbol{x}_{n+1}$) can meet the nonreactive rectification body of the rectifying section in Figure 13b. Once we increase the heat duty, the shortcut algorithm should continue from step 4 to determine a suitable *Da*.

Extension of the Shortcut Method for Columns with Reactive Trays in Both Sections

If the 2-pentene decomposition occurs within the whole column, that is, in both rectifying and stripping sections, we can extend the shortcut method for one section into this case. Given the product compositions and the heat duty, the reactive pinch points of both sections are determined. For specified Damköhler numbers Da^r and Da^s in the rectifying and stripping sections, the unstable eigenvectors at the pinch points are calculated. These eigenvectors are used to approximate the column profiles, as previously presented. The liquid and vapor compositions at the feed stage are identical to the intersection points of the estimated liquid and vapor profiles for the rectifying and stripping sections in Figure 14. In order to guarantee feasible operation, it should be checked whether the sum of the reaction extents for the two sections is equal to an overall reaction extent. For the fixed vapor composition at the feed stage, the total cascade difference point for the rectifying section (δ_l^r) and the final liquid com-

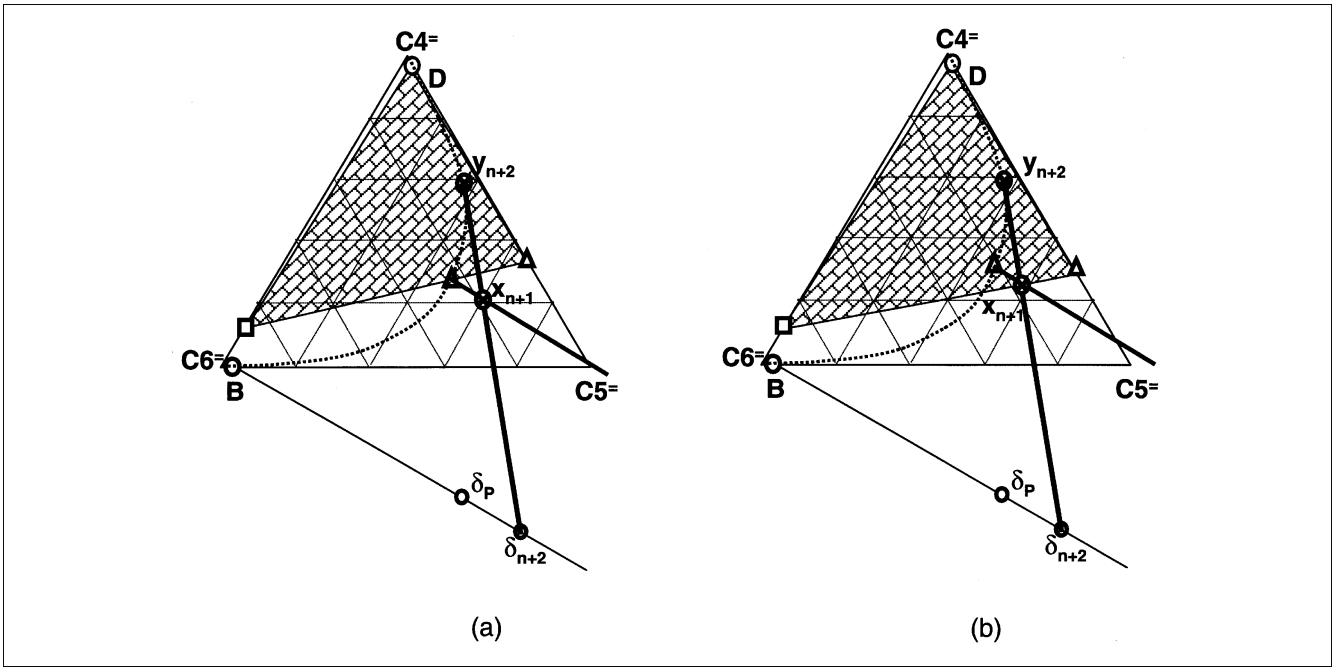

Figure 13. Increasing the reflux ratio when the final liquid composition (x_{n+1}) does not touch the nonreactive rectification body.

(a) No intersection between $\boldsymbol{x}_{n+1}$ and the nonreactive rectification body at reflux ratio $= 1.5$. (b) Intersection between $\boldsymbol{x}_{n+1}$ and the nonreactive rectification body at reflux ratio $= 1.67$.

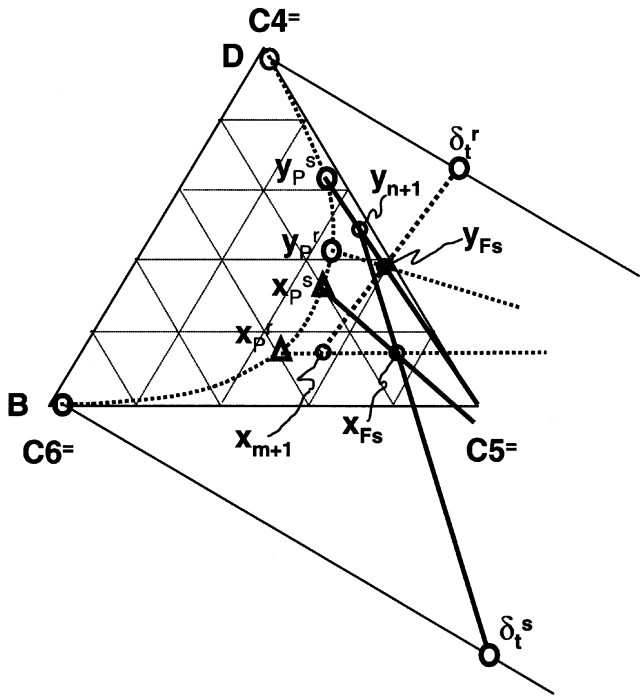

Figure 14. Geometrical construction of a shortcut method for reaction in both sections.

The dotted lines represent the rectifying section and the solid lines denote stripping section.

position of the rectifying section ($\boldsymbol{x}_{m+1}$) are simultaneously determined on the cascade difference point trajectory and on the estimated liquid profile. In the same way, we can obtain the total cascade difference point for the stripping section (δ_t^s) and the final vapor composition of the stripping section ($\boldsymbol{y}_{m+1}$) from the fixed liquid composition at the feed stage. Thus, we calculate the sum of two reaction extents (ξ_t^r and ξ_t^s) from these two cascade difference points and check if this sum equals the total reaction extent calculated from the overall material balance.

Therefore, we propose the algorithm of a shortcut method for the case of both reactive sections:

(1) Specify a column pressure and give the feed and product specifications.

(2) Set a heat duty of the condenser or reboiler.

(3) Obtain the reactive pinch points of each reactive section.

(4) Choose Da^r and Da^s.

(5) Calculate the eigenvectors at the pinch and approximate the reactive liquid and vapor composition profiles for the rectifying and stripping sections.

(6) If the profiles do not intersect, choose different Da's and go to step 5. If the profiles do not intersect for any choice of Da^r and Da^s, increase or decrease the heat duty and go to step 3.

(7) From the intersection points on the two liquid profiles and the two vapor profiles, determine the total cascade difference points for the stripping section (δ_t^s) and the rectifying section (δ_t^r) and calculate the reaction extents for both sections (ξ_t^r and ξ_t^s).

Table 2. Results for Q_B and Da from the Shortcut Method and AspenPlus for the 2-pentene Decomposition Reaction

Reaction Zones	Shortcut Method*	AspenPlus**
Stripping section: Q_B(MJ/s)/Da	55.07/0.0180	55.06/0.0346
	43.33/0.0750	43.52/0.0487
	31.59/0.3200	31.51/0.3325
Rectifying section: Q_B(MJ/s)/Da	55.07/0.0600	55.06/0.1403
	43.33/0.2400	43.27/0.3700
	38.64/0.9700	38.58/0.7744
Both sections (all reactive):	31.59/0.0250	31.51/0.0448
Q_B(MJ/s)/Da	29.24/0.0750	29.13/0.0750

*,**Feed and product specifications: F = 1.0 kmol/s, D = B = 0.5 kmol/s, $\boldsymbol{x}_F$ = [0.0 1.0 0.0], $\boldsymbol{x}_D$ = [0.98 0.01992 0.00008] and $\boldsymbol{x}_B$ = [0.00008 0.01992 0.98] for $C_4^=$, $C_5^=$ and $C_6^=$.

**25 reactive stages and 25 nonreactive stages for rectifying and stripping sections, 50 reactive stages for both reaction sections including a condenser (1st stage) and a reboiler (50th stage).

(8) Compare the sum of ξ_t^r and ξ_t^s with the total reaction extent (ξ_t). If this sum is less than the total reaction extent, return to step 4 and try other Da's. If $\xi_t^r + \xi_t^s < \xi_t$ for any choice of Da^r and Da^s, increase the heat duty and go to step 3.

Results for the 2-pentene Decomposition Reactive System

Table 2 summarizes the results from the shortcut method and compares these results with simulation results from Aspen Plus for identical feed and product compositions. The feed contains pure 2-pentene and its flow rate is 1 kmol/s. The flow rates for the top and bottom products are 0.5 kmol/s for all three cases. The feed and product streams are all saturated liquids. For all simulations, the required distillate and bottoms compositions have been chosen as $\boldsymbol{x}_D$ = [0.98, 0.01992, 0.00008] and $\boldsymbol{x}_B$ = [0.00008, 0.01992, 0.98] for $C_4^=$, $C_5^=$ and $C_6^=$. While carrying out Aspen simulations, we change molar stage holdups (Damköhler numbers) for nearly the same heat duties until we get the identical product specification. Here, we also iterate with different numbers of reactive or nonreactive stages and select 50 stages to obtain feasible product specs for the three cases of reaction locations in Table 2.

Let's first focus on the results from the shortcut method in Table 2. The Damköhler numbers for the reactive stripping section are smaller than those for the reactive rectifying section. For example, the Damköhler number of the stripping section is $Da = 0.3200$ at the reboiler duty of $Q_B = 31.59$ MJ/s, while $Da = 0.97$ in the rectifying section at the reboiler duty of $Q_B = 38.64$ MJ/s. Therefore, the stripping section displays better reaction performance than the rectifying section since the reaction holdup ($Da = 0.3200$) for the reactive stripping section is smaller than that ($Da = 0.97$) for the reactive rectifying section with the lower reboiler duty.

Furthermore, if we consider a column where all stages are reactive, the Damköhler numbers are even smaller than those for the two cases of reaction occurring only in either the rectifying or the stripping section. For the reboiler heat duty, 31.59 MJ/s, Da is 0.0250 for all reactive sections and 0.3200 for the stripping reaction zone. Thus, this case has the best performance in terms of the smallest column dimension or catalyst amount. Aspen simulation results show the same trend for column performance indicating reaction in both

sections has the lowest Damköhler number for smaller reboiler duties. The Damköhler numbers obtained from the shortcut method are used as the initialization for the rigorous Aspen simulations. There is a good agreement between the shortcut results and the Aspen simulation results in Table 2.

Application of the Shortcut Method to the Methyl Acetate Production System

Methyl acetate (MA) is produced by the dehydration reaction of methanol (MT) and acetic acid (AC) using an acid catalyst

$$CH_3COOH(AC) + CH_3OH(MeOH) \leftrightarrow CH_3COOCH_3(MA) + H_2O(W) \quad (9)$$

Its kinetics is obtained from Xu and Chuang (1996) and Mazzotti et al. (1997) and summarized in the appendix. There are two minimum boiling azeotropes, Water-MA and MT-MA at 1 atm.

Figure 15 shows two possible liquid compositions (x_{m+1}'s) of the final reactive stage intersecting the nonreactive rectification body of the stripping section (tetrahedron). Using these two final liquid compositions, we can satisfy the necessary condition for the feasible split in terms of intersection between the reactive profile and the nonreactive rectification body of the stripping section. Then, the heat and material balances will determine the lowest *Da* for any estimated liquid and vapor profiles with $0 \le Da \le 1{,}000$. This is the same way as for the previous ternary system in Figure 12 except two possible final liquid compositions. Here, the final stage means the lowest reactive stage in the rectifying section and the accumulated reaction extent (ξ_{m+1}) from the top to this final stage satisfies the overall reaction extent (ξ_t). The heat balance around the rectifying envelope also determines one final liquid composition from these two final liquid compositions (x_{m+1}'s). y_{m+2} in Figure 15 is the vapor composition coming up to the final stage $(m+1)$ in Figure 11.

Table 3. Results for Q_B and *Da* from the Shortcut Method and AspenPlus for the Methyl Acetate Production

Reaction Zones	Shortcut Method*	AspenPlus**
Stripping section:	81.13/0.0625	81.39/0.0626
Q_B(MJ/s)/*Da* range	64.80/0.0550	65.05/0.0575
	38.67/0.1650	38.85/0.1579
Rectifying section:	81.13/1.6000	81.43/1.4379
Q_B(MJ/s)/*Da* range	64.80/1.3800	65.06/1.3252
	38.67/0.6270	38.90/1.1842
Both sections (all reactive):	39.98/0.2980	38.74/0.1241
Q_B(MJ/s)/*Da* range	38.67/0.3250	35.56/0.1353

*,**Feed and product specifications : F = 2.0 kmol/s, D = B = 1.0 kmol/s, x_F = [0.5 0.5 0.0 0.0], x_D = [0.0002 0.4882 0.5068 0.0048] and x_B = [0.49 0.002 0.003 0.505] for AC, MT, MA and W.

**30 reactive stages and 30 nonreactive stages for rectifying and stripping sections, 60 reactive stages for both reaction sections including a condenser (1st stage) and a reboiler (60th stage).

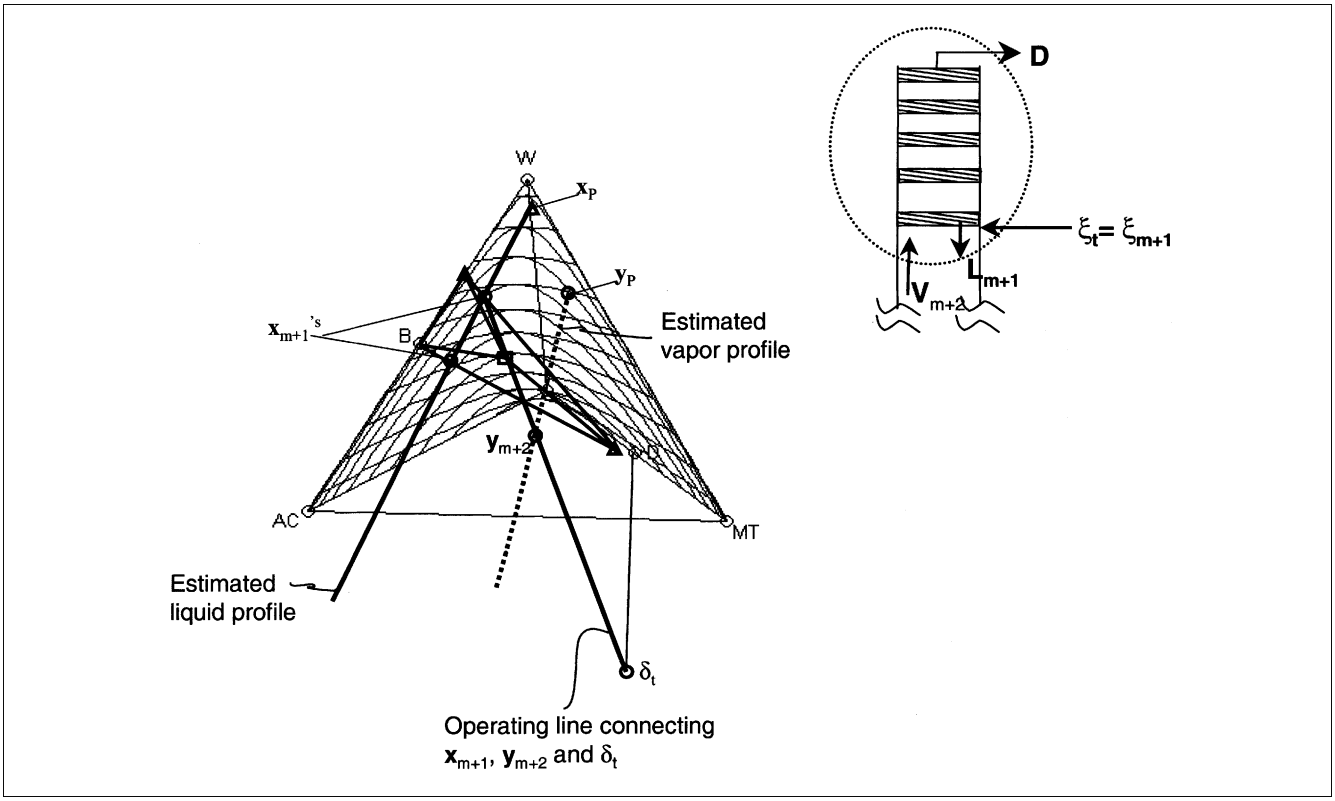

Figure 15. Geometrical construction of a shortcut method for the reactive rectifying section in the methyl acetate quaternary system.

The tetrahedron inside the tetrahedral composition simplex is the nonreactive rectification body for the stripping section.

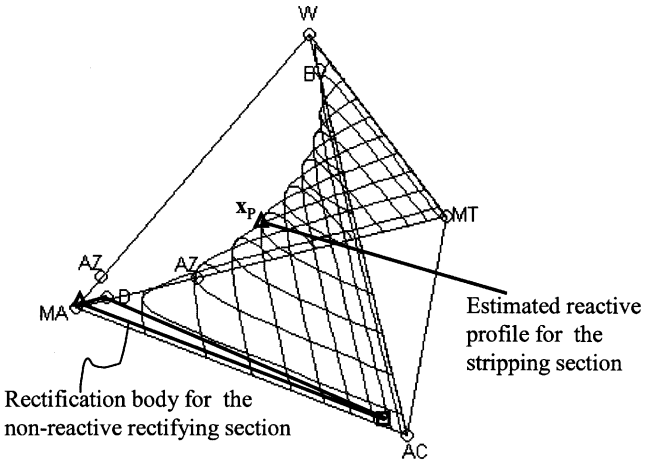

Figure 16. No intersection between the reactive profile of the stripping section and the nonreactive rectification body of the rectifying section.

x_F = [0.5, 0.5, 0.0, 0.0], x_D = [0.005, 0.068, 0.912, 0.015] and x_B = [0.08, 0.017, 0.003, 0.9] for AC, MT, MA and W. All feed and product streams are saturated liquid. External reflux ratio = 2.0.

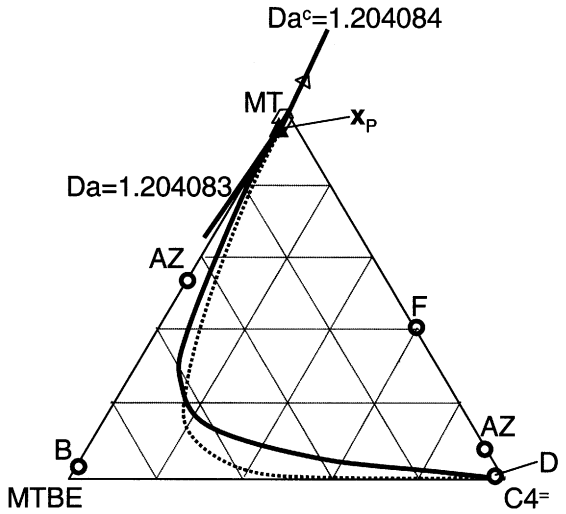

Figure 18. Limiting composition profile of the reactive rectifying section with Da^c.

x_F = [0.4, 0.6, 0.0], x_D = [0.003, 0.985, 0.012] and x_B = [0.023425, 0.007875, 0.9687] for MT, $C_4^=$ and MTBE. All feed and product streams are saturated liquid. External reflux ratio = 15.0. Flow rates: F/D/B = 1.0/0.21/0.4 kmol/s. The arrow is the unstable eigenvector direction of the pinch point.

Table 3 shows the results from the shortcut method and the Aspen Plus simulations. The *Da*'s estimated from the shortcut method reasonably match the *Da*'s calculated from Aspen Plus. The shortcut results show that *Da*'s for the stripping reaction zone are smaller than those for the rectifying reactive section under the same heat duty. For the same heat duty, Q_B = 81.13 MJ/s, Da = 0.0625 is for the stripping section, and Da = 1.6000 is for the rectifying section. So, the stripping reactive section is more efficient than the rectifying reactive section in terms of smaller catalyst holdups. The Aspen Plus results also support this fact: *Da*'s are 0.0626 and 1.4379 for the stripping section and the rectifying section, respectively, for Q_B = 81.39 MJ/s and Q_B = 81.43 MJ/s. When both sections are reactive, *Da* is 0.325 for Q_B = 38.67 MJ/s in the shortcut results. This is larger than Da = 0.165 for the stripping reaction zone under the identical reboiler duty. In the Aspen Plus results, the *Da*'s for all reactive case and the stripping section are 0.1353 and 0.1579 for Q_B = 38.74 MJ/s and Q_B = 38.85 MJ/s. In these Aspen simulations, 60 stages are reactive for the all-reactive case, and 30 reactive stages for the case of only a stripping reactive section. So, in terms of 30 reactive stages, the case of both reactive sections has Da = 0.2706 (= 0.1353*2) to make fair comparison. So the stripping reaction zone has the best performance in terms of the lowest catalyst holdups.

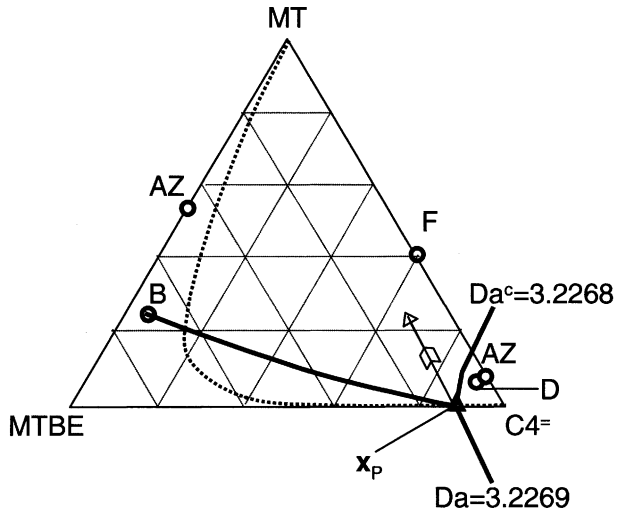

Figure 17. Limiting composition profile of the reactive stripping section with Da^c in the MTBE production system.

The dotted curve connecting MT and $C_4^=$ denotes reaction equilibrium at 8 atm. x_F = [0.4, 0.6, 0.0], x_D = [0.053, 0.9208, 0.0262] and x_B = [0.233925, 0.06138, 0.704695] for MT, $C_4^=$ and MTBE. All feed and product streams are saturated liquid. External reflux ratio = 15.0. Flow rates: F/D/B = 1.0/0.31/0.4 kmol/s. Bifurcation occurs at x_P. The arrow is the unstable eigenvector direction of the pinch point.

Another important application of the shortcut method is to investigate whether a single-feed distillation column can produce pure methyl acetate at a higher reaction extent. Figure 16 clearly shows that for a given distillate composition with 91.2% of methyl acetate, the nonreactive rectification body of the rectifying section does not intersect the estimated reactive profile of the stripping section. Hence, it is infeasible to obtain this top product. Further increasing the methyl acetate purity in the top product makes the nonreactive rectification body reduce to a straight line connecting AC and MA vertices. No intersection between this nonreactive rectification body and the reactive profile is found as the MA purity increases in the top product. With different reflux ratios (from 0.7 to 10) for the same distillate composition as in Figure 16, there is no intersection between the nonreactive rectification body and the reactive profile. Even with a rectifying reaction

zone or with all reactive stages of the whole column, it is confirmed by the shortcut method that a single-feed reactive distillation column cannot produce pure methyl acetate. This is why a double-feed distillation column should be employed to obtain pure methyl acetate (Agreda and Partin, 1984).

Applying a Shortcut Method to the Nonisomolar MTBE Reactive System

One mole of methyl *tert*-butyl ether (MTBE) is produced from one mole of iso-butene ($C_4^=$) and one mole of methanol (MT). Two minimum boiling azeotropes exist at 8 atm: one is between MT and $C_4^=$ and the other is between MT and MTBE (See "AZ" in Figure 17). The reaction consumes two moles of the reactants for every mole of the product that it yields. The kinetic data are collected in the appendix. The geometry for this nonisomolar reaction in the original composition space is different from the previous two iso-molar reactions. The reaction difference point (Hauan et al., 1996; Hugo, 1965; Stichlmair and Fair, 1998) is finite and $\delta_R = [1\ 1\ -1]^T$ for MT, $C_4^=$, and MTBE, respectively, while the isomolar reactions have infinite reaction difference points.

For this nonisomolar MTBE reaction, the limiting composition profiles with Da^c's are also available in Figures 17 and 18. The kinetic data are collected in the appendix. The unstable eigenvector direction of the stripping pinch point does not match well with the calculated limiting composition with $Da^c = 3.2268$ in Figure 17. For the rectifying reaction zone in Figure 18, the limiting composition profile ($Da^c = 1.204084$) after the pinch point ($\boldsymbol{x}_P$) lies outside the valid composition simplex. This unusual behavior may come from the nonisomolar stoichiometry of the MTBE reaction or nonideal phase equilibrium, but the correct reason for this is still unknown. Due to these behaviors of the composition profiles, the shortcut procedures presented in the last sections cannot be applied. However, the MTBE system can be addressed if the behavior of the limiting composition profiles are combined with geometrical insights.

For the stripping reaction zone, the reaction extent from the bottom to the pinch point is always negative if a straight line connects the pinched vapor and liquid compositions ($\boldsymbol{x}_P$ and $\boldsymbol{y}_P$) in Figure 19. This straight line intersects the cascade difference point trajectory at the left extension of the bottom product composition, where the reaction extent is negative according to the following cascade difference point definition (Hauan et al., 2000a; Lee et al., 2001a). In this equation, the sum of stoichiometric coefficients (ν_T) is -1

$$\boldsymbol{\delta}_P = \frac{B\boldsymbol{x}_B - \nu_T \boldsymbol{\delta}_R \xi_P}{B - \nu_T \xi_P} \tag{10}$$

Therefore, the liquid composition at the final reactive stage starting from the bottom must lie somewhere between $\boldsymbol{x}_P$ and the MT$-C_4^=$ binary edge in order to have an overall positive reaction extent like the composition profile with $Da^c = 3.2268$ in Figure 17. The necessary condition for the feasibility is that the final liquid composition of the reactive profile should intersect the nonreactive rectification body of the rectifying section. So, this final liquid composition ($\boldsymbol{x}_{n+1}$ in Figure 11) is geometrically confined between two points on the upper edge of the nonreactive rectification body, as shown in Figure 20. One point is the intersection between the edge of the rectification body and the straight line connecting the bottom composition ($\boldsymbol{x}_B$) and the pinched vapor composition ($\boldsymbol{y}_P$). The other point is the intersection between the edge of the rectification body and the line joining the total cascade difference point (δ_t) and the pinched vapor composition ($\boldsymbol{y}_P$). If the final liquid composition of the reactive profile is at intersection I in Figure 20, then the reaction extent from the bottom to stage $n+2$ is zero because δ_P is equal to $\boldsymbol{x}_B$ in Eq. 10. If it is at intersection "II" in Figure 20, then the reaction extent from the bottom to stage $n+2$ is equal to the total reaction extent. Thus, the final liquid composition is confined by two limiting cases of the reaction extents: the first case of total reaction (maximum Da) on the final stage (stage $n+1$) at intersection I and the second case of zero reaction ($Da = 0$) on the final stage at intersection II. Note that the pinched vapor composition ($\boldsymbol{y}_P$) is used to obtain this range of the

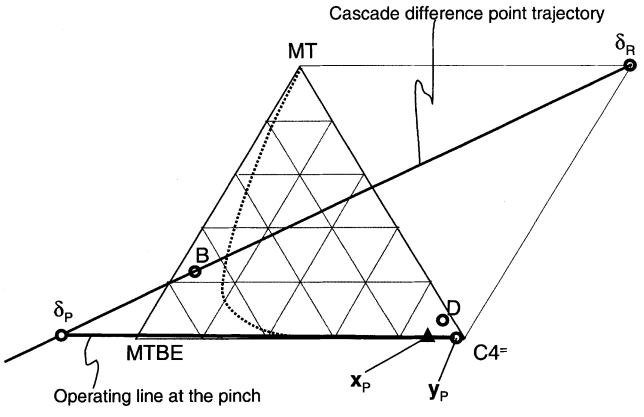

Figure 19. Negative reaction extent at the pinch point for the reactive stripping section in the MTBE production system.

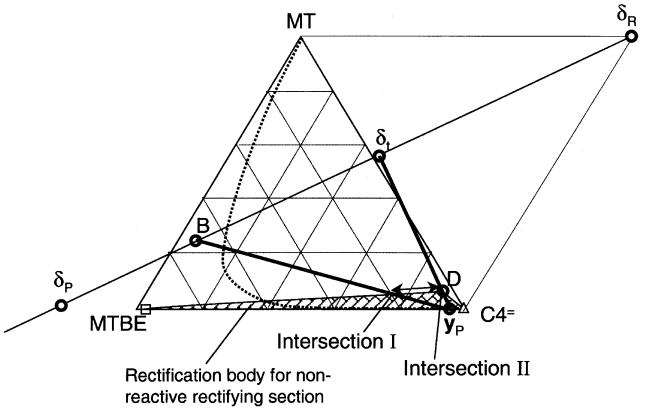

Figure 20. Determination of the liquid composition at the final reactive stage of the stripping section.

The both-ended arrow between intersections I (zero reaction extent) and II (total reaction extent) is the possible range for the final liquid composition ($\boldsymbol{x}_{n+1}$).

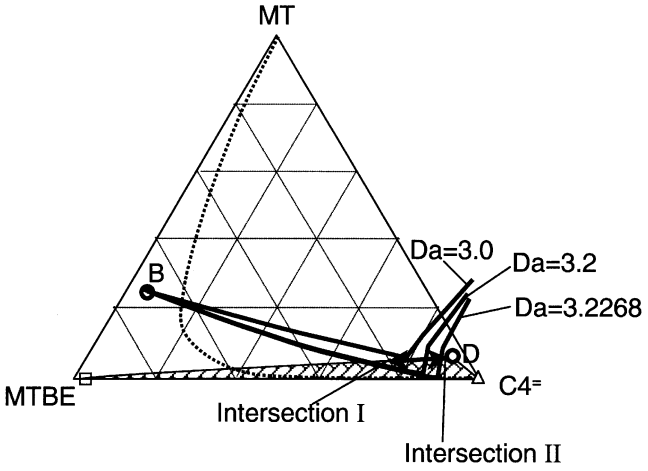

Figure 21. Calculated composition profiles of the reactive stripping section.

All conditions are identical to Figure 17 except Damköhler numbers.

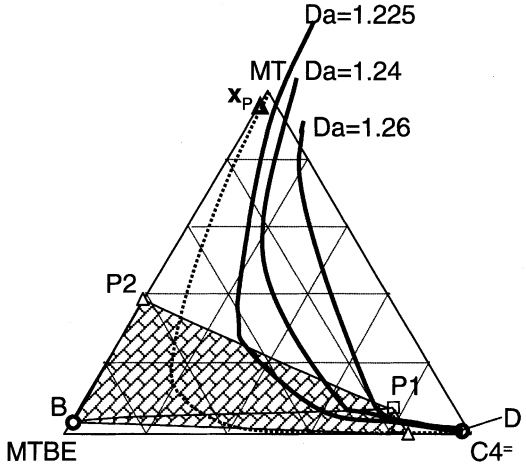

Figure 23. Manifold of reactive stage profiles with nearly identical *Da*'s passing through the P1-P2 edge of the nonreactive rectification body of the stripping section.

final liquid composition because this information is accessible without any tray calculations.

To develop a shortcut algorithm, the middle point of these two intersections is taken as the final liquid composition ($\boldsymbol{x}_{n+1}$) because the calculated composition profiles in Figure 21 passing through this interval (between I and II) do not have significantly different values of *Da*'s. The vapor composition profile after the pinch point can be confined to the straight line connecting the pinched vapor composition and the equilibrated vapor composition with the final liquid composition. For the given final liquid composition ($\boldsymbol{x}_{n+1}$), the internal reboil ratio calculated from the heat balance determines the cascade difference point at stage $n+2$ on the cascade difference point trajectory and the vapor composition at stage $n+2$ on the estimated vapor profile. These two cascade difference points (δ_{n+1} and δ_{n+2}) yield two reaction extents (ξ_{n+1} and ξ_{n+2}) for given bottom product composition and flow rate. From the difference in the reaction extents between stage $n+2$ and stage $n+1$ ($\xi_{n+1}-\xi_{n+2}$), we can calculate *Da* with Eq. 11. Note that ($\xi_{n+1}-\xi_{n+2}$) is the net reaction extent at stage $n+1$. The detailed derivation is available in the appendix

$$Da = \frac{\xi_{n+1} - \xi_{n+2}}{\left(F/k_{f,\mathrm{ref}}\right) * r_{n+1}} \tag{11}$$

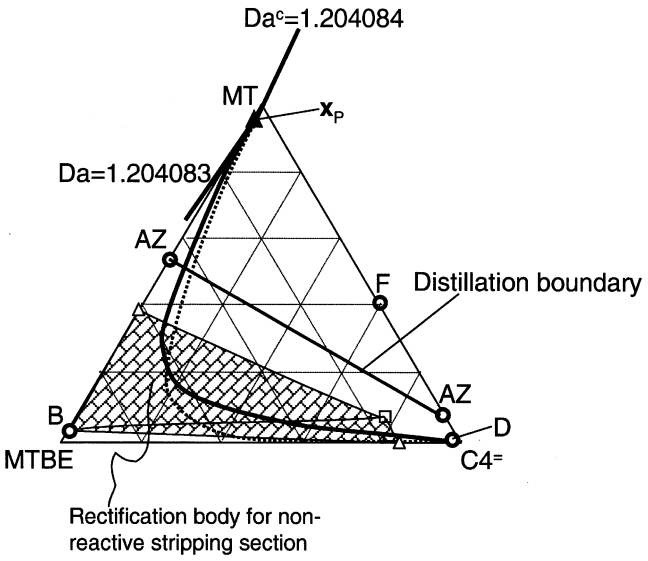

Figure 22. Limiting composition profile of the reactive rectifying section and the nonreactive rectification body for the stripping section. All conditions are identical to Figure 18.

As already shown in Figure 18, the limiting composition profile with Da^c for the reactive rectifying section partly lies within the reverse reaction zone. It also lies in the different distillation region from the region where the nonreactive rectification body of the stripping section is placed in Figure 22. So, using composition profiles with Da^c's for a shortcut algorithm does not result in a feasible column since the overall reaction extent is not satisfied.

However, if *Da* slightly increases from the critical value in Figure 23, the composition profiles lie only in the forward reaction zones, as shown in Figure 23. The composition profiles are quite different according to small deviations in *Da*'s (1.225 to 1.26) like the previous ones in Figure 3. However, all of the composition profiles touch the nonreactive rectification body of the stripping section. The reaction extent increases as the composition profiles proceed toward the upper edge of P1-P2 starting from the top product (D) since those profiles lie within the forward reaction region in Figure 23. Thus, this edge (P1-P2) can be the place for the potential final liquid composition of the reactive rectifying section ($\boldsymbol{x}_{m+1}$) since the final liquid composition should intersect the nonreactive rectification body. The middle point of P1-P2 edge is chosen as the final liquid composition satisfying the overall reaction conversion, because all of the positions on

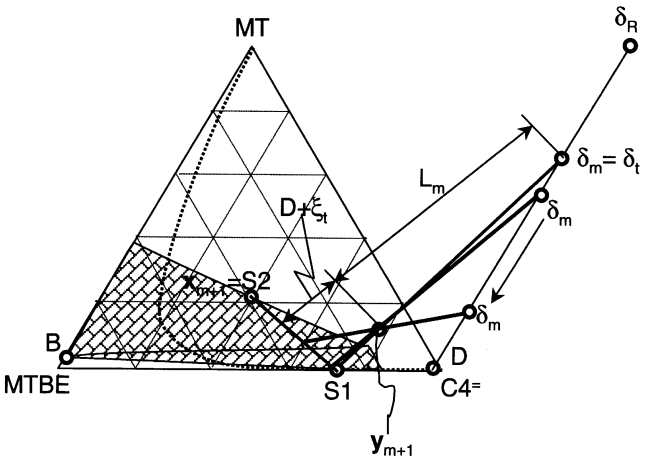

Figure 24. Range of the liquid composition (x_m) and the cascade difference point (δ_m) at stage m.

The straight line connecting S1 ($Da = 0$) and S2 (Da = very high) is the range for x_m.

the P1-P2 edge correspond to nearly identical Da's (1.225 to 1.26) from the calculated composition profiles in Figure 23. Then, we calculate the equilibrated vapor composition (y_{m+1}) with this final liquid composition (x_{m+1}). To determine Da's, one stage calculation is performed from stage $m+1$ to stage m for this given vapor composition. So, the possible range for the liquid composition at stage m (x_m) should be determined.

A simple trick is taken here to place the range of this liquid composition (x_m). First, if the overall reaction extent is satisfied at this stage m, we can roughly calculate the internal reflux ratio ($r_m = L_m$/D) for a given external reflux ratio without considering heat balance. For example, if the external reflux is fixed as 15D and overall reaction conversion is $\xi_t = 1.8571$D calculated from feed and product specifications, then the internal reflux ratio is (15D-1.8571D)/D, as in Figure 24, when the overall reaction extent is satisfied at stage m ($\delta_m = \delta_t$). So, the liquid composition at stage m is located on the lower-left extension of the straight line connecting the total cascade difference point and the vapor composition at stage $m+1$ according to the ratio of $L_m/(D + \xi_t) =$ 13.1429D/2.8571D (refer to S1 in Figure 24). Then, this liquid composition at stage m is confined to the straight line connecting the previous position (S1) and the final liquid composition x_{m+1} (S2). The Damköhler number is zero when x_m lies at the position of S1 since δ_m is identical to $\delta_t = \delta_{m+1}$ and the difference of the two reaction extents ($\xi_t - \xi_m$) becomes zero. As the liquid composition (x_m) moves from S1 to S2, the Damköhler number increases and the cascade difference point (δ_m) moves from (δ_t) to x_D, as shown in Figure 24. The heat balance simultaneously determines the position of x_m on the line of S1-S2 and that of δ_m on the trajectory of cascade difference points. Once the position of δ_m is determined, the corresponding reaction extent (ξ_m) is calculated for given top composition and flow rate. The difference between two reaction extents ($\xi_t - \xi_m$) will give the Damköhler number in the same way as in Eq. 11 for the reactive stripping section.

Table 4 summarizes the results obtained from the shortcut method. The rectifying reaction zone has smaller Da's and heat duties than the stripping reaction zone even for the higher overall reaction extent and purer top and bottom products. Thus, the rectifying reaction zone outperforms the stripping reaction zone. This result is consistent with the previous result obtained by the geometrical analysis in Lee and Westerberg (2001a). The Da's calculated from the shortcut method are not much different from those by the boundary value method and can be used as the initialization of rigorous calculations.

One important design insight from the shortcut procedure is that the reactive stripping section cannot yield the same product specification as in the reactive rectifying section. In a column with the reactive stripping section, the nonreactive rectification body of the rectifying section shrinks into the line connecting the node pinch near the MTBE vertex and x_D as in Figure 25. Thus, this nonreactive rectification body can intersect some liquid compositions lying on the reaction equilibrium curve. If we select the pinched liquid composition (x_P) as this intersection, this pinched composition is the final liquid composition (x_{n+1}) of the reactive stripping section. Since this pinch composition lies on the reaction equilibrium curve, the reaction rate, r_{n+1} is zero and the Da becomes mathematically infinite according to Eq. 11. Thus, it is impossible to produce pure MTBE and $C_4^=$ when the reaction occurs in the stripping section. The approach suggested in this article confirms the results reported by other authors (Preston, 1998; Smith 1981, 1992). Hence, the method can be used in other cases where in depth information about suitable column configurations is not given.

Table 4. Results for Q_B and Da from the Shortcut Method and the Boundary Value Method (BVP) for the MTBE Production

Reaction Zones	Shortcut Method	BVP
Stripping section: Q_B(MJ/s)/Da		
x_F = [0.4 0.6 0.0] for MT, $C_4^=$ and MTBE	113.58/4.5509	113.58/3.6700 (9)*
x_D = [0.0530 0.9208 0.0262]	96.28/4.3781	96.28/3.4440 (9)*
x_B = [0.233925 0.06138 0.704695]	84.75/3.9891	84.75/3.2266 (11)*
F/D/B = 1.0/0.31/0.4 kmol/s → ξ_t = 0.29 kmol/s		
Rectifying section:		
Q_B(MJ/s)/Da range		
x_F = [0.4 0.6 0.0] for MT, $C_4^=$ and MTBE	68.78/1.3521	68.78/1.5670 (6)*
x_D = [0.003 0.985 0.012]	57.61/1.3237	57.61/1.3620 (6)*
x_B = [0.023425 0.007875 0.9687]	50.16/1.4349	50.16/1.2250 (6)*
F/D/B = 1.0/0.21/0.4 kmol/s → ξ_t = 0.39 kmol/s		

*Number in parentheses shows reactive stages in each section.

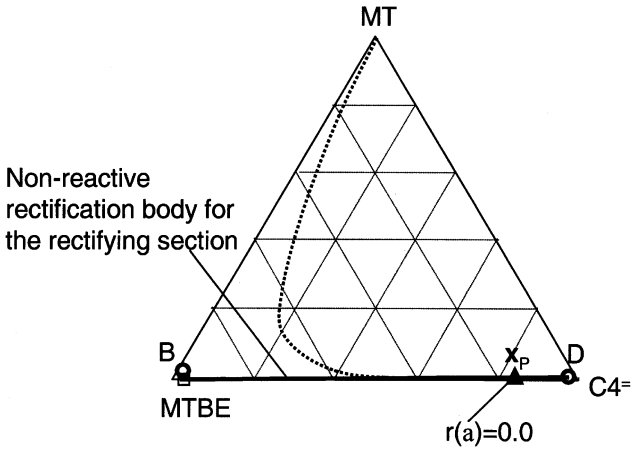

Figure 25. Infeasibility of the reactive stripping section to produce pure MTBE and $C_4^=$.

The feed and product specifications are the same as in Figure 18.

Conclusions

In this article, a new shortcut method has been derived to analyze and design reactive distillation systems. This new procedure is based on the nonreactive rectification body method, the critical composition profiles, the analysis of the eigenvectors of pinch points, and geometrical design insights. For the isomolar reactive systems ($2B \leftrightarrow A + C$ and $A + B \leftrightarrow C + D$), the unstable eigenvector directions are directly used for column profile estimations. For the nonisomolar reactive system ($A + B \leftrightarrow C$), geometrical consideration is implemented with the concept of cascade difference points to calculate reaction holdups (*Da*'s). Even though the position of pinch points and the eigenvector directions differ depending on the phase equilibrium among reactive mixtures, the developed algorithm can be applied to most types of single isomolar or nonisomolar reaction. The limitation of this shortcut method is that the number of nonreactive or reactive stages is not directly calculated even if the shortcut results (*Da*'s and energy requirements) will guide or help the rigorous calculations to determine this design parameter.

In the future, we will extend our algorithms into multireaction and multifeed/product systems by using visualization insights (Lee, 2002; Pisarenko et al., 2001; Stichlmair and Fair, 1998) and the proposed pinch point analysis. To overcome visual limitations for multireaction systems, the reaction extents determined in the unstable eigenvector can be used for developing a general shortcut method.

Acknowledgment

J. W. Lee is grateful for the support of Alexander van Humboldt Foundation, Professional Staff Congress City University of New York (PSC-CUNY), and American Chemical Society—Petroleum Research Fund (ACS-PRF, G). This work was also partially supported by Deutsche Forschungsgemeinschaft (DFG).

Notation

B = molar bottom product flow rate
$\boldsymbol{c}_P$ = normalized product coefficient vector
$\boldsymbol{c}_R$ = normalized reactant coefficient vector
C = number of components
D = molar distillate flow rate
Da = Damköhler number, $(\mathrm{Hk}_{f,\mathrm{ref}})/F$
Da^c = critical Damköhler number
F = molar feed flow rate
H = reaction molar holdup on each stage
k_f = forward reaction rate constant
$k_{f,\mathrm{ref}}$ = forward reaction rate constant at the reference temperature
L_m = molar liquid flow rate at stage m in the rectifying section
L_n = molar liquid flow rate at stage n in the stripping section
L_P = molar liquid flow rate at the reactive pinch point
N_R = number of reaction
Q_B = reboiler heat duty
r_i = reaction rate at stage i
s = internal reboil ratio at the pinch
T = temperature
T_{n+1} = temperature at stage $n+1$
T_P = temperature at a pinch point
V_m = molar vapor flow rate at stage m in the rectifying section
V_n = molar vapor flow rate at stage n in the stripping section
V_P = molar vapor flow rate at the reactive pinch point
$\boldsymbol{x}_B$ = bottom product composition
$\boldsymbol{x}_D$ = distillate composition
$\boldsymbol{x}_F$ = feed composition
$\boldsymbol{x}_{Fs}$ = the liquid composition at the feed stage
$\boldsymbol{x}_m$ = liquid composition at stage m in the rectifying section
$\boldsymbol{x}_n$ = liquid composition at stage n in the stripping section
$\boldsymbol{x}_P$ = liquid composition at the reactive pinch point
$\boldsymbol{x}_P^r$ = pinched liquid composition in the rectifying section
$\boldsymbol{x}_P^s$ = pinched liquid composition in the stripping section
$\boldsymbol{y}_{Fs}$ = vapor composition at the feed stage
$y_i^*(\boldsymbol{x},T)$ = vapor composition in equilibrium with liquid composition $\boldsymbol{x}$ at temperature T
$\boldsymbol{y}_m$ = vapor composition at stage m in the rectifying section
$\boldsymbol{y}_n$ = vapor composition at stage n in the stripping section
$\boldsymbol{y}_P$ = vapor composition at the reactive pinch point
$\boldsymbol{y}_P^r$ = pinched vapor composition in the rectifying section
$\boldsymbol{y}_P^s$ = pinched vapor composition in the stripping section

Greek letters

δ_m = cascade difference point at stage m in the rectifying section
δ_P = cascade difference point at the reactive pinch point
δ_n = cascade difference point at stage n in the stripping section
δ_R = reaction difference point
δ_t = total cascade difference point
δ_t^r = total cascade difference point for the reactive rectifying section
δ_t^s = total cascade difference point for the reactive stripping section
$\boldsymbol{\nu}$ = reaction coefficient vector
$\boldsymbol{\nu}_i$ = reaction coefficient for component i
$\boldsymbol{\nu}_T$ = total sum of reaction coefficients
ξ_m = accumulated reaction extent from the top to stage m in the rectifying section
ξ_P = accumulated reaction extent from the top or the bottom to the reactive pinch point
$\xi_{r,n}$ = accumulated reaction extent for reaction r from the bottom to stage n
$\xi_{r,P} = \xi_P$ for reaction r
ξ_n = accumulated reaction extent from the bottom to stage n in the stripping section
ξ_t = overall reaction extent in a column
ξ_t^r = overall reaction extent for the reactive rectifying section
ξ_t^s = overall reaction extent for the reactive stripping section

Literature Cited

Agreda, V. H., and L. R. Partin, "Reactive Distillation Process for The Production of Methyl Acetate," U.S. Patent No. 4,435,595 (1984).

Barbosa, D., and M. F. Doherty, "Design and Minimum-reflux Calculations for Single-feed Multicomponent Reactive Distillation Columns," *Chem. Eng. Sci.*, **43**, 1523 (1988a).
Barbosa, D., and M. F. Doherty, "Design and Minimum-reflux Calculations for Double-feed Multicomponent Reactive Distillation Columns," *Chem. Eng. Sci.*, **43**, 2377 (1988b).
Bausa, J., v. Watzdorf, and W. Marquardt, "Shortcut Method for Non-ideal Multicomponent Distillation: 1. Simple Columns," *AIChE J.*, **44**, 2181 (1998).
Bausa J., "Näherungsverfahren für den konzeptionellen Entwurf und die thermodynamische Analyse von destillativen Trennprozessen," *Fortschr.-Ber. VDI*, Reihe 3, **Nr. 692** (2001).
Buzad, G., and M. F. Doherty, "Design of Three-component Kinetically Controlled Reactive Distillation Columns Using Fixed-point Methods," *Chem. Eng. Sci.*, **49**, 1947 (1994).
Chadda, N., M. F. Malone, and M. F. Doherty, "Feasible Products for Kinetically Controlled Reactive Distillation of Ternary Mixtures," *AIChE J.*, **46**, 923 (2000).
Doherty, M. F., and G. Buzad, "Reactive Distillation by Design," *Trans. Inst. Chem. Eng.*, **70**, 448 (1992).
Edgar, T. F., "Process Information: Achieving a United View," *Chem. Eng. Prog.*, **96**(1), 51 (2000).
Hauan, S., T. Omtveit, and K. M. Lien, "Analysis of Reactive Separation Systems," paper 5f, AIChE Meeting, Chicago (Nov. 1996).
Hauan, S., A. R. Ciric, A. W. Westerberg, and K. M. Lien, "Difference Points in Extractive and Reactive Cascades. I - Basic Properties and Analysis," *Chem. Eng. Sci.*, **55**, 3145 (2000a).
Hauan, S., A. W. Westerberg, and K. M. Lien, "Phenomena Based Analysis of Fixed Points in Reactive Separation Systems," *Chem. Eng. Sci.*, **55**, 1053 (2000b).
Hendershot, D. C., "Process Minimization: Making Plants Safer," *Chem. Eng. Prog.*, **96**(1), 35 (2000).
Hugo, P., "Die Berechnung des chemischen Umsatzes von Mehrkomponenten-Gasgemischen an porösen Katalysatoren," *Chem. Eng. Sci.*, **20**, 187 (1965).
Keller, G. E., and P. F. Bryan, "Process Engineering: Moving in New Directions," *Chem. Eng. Prog.*, **96**(1), 41 (2000).
Julka, V., and M. F. Doherty, "Geometric Behavior and Minimum Flows for Nonideal Multicomponent Distillation," *Chem. Eng. Sci.*, **45**, 1801 (1990).
Lee, J. W., S. Hauan, and A. W. Westerberg, "Extreme Conditions in Binary Reactive Distillation," *AIChE J.*, **46**, 2225 (2000).
Lee, J. W., and A. W. Westerberg, "Graphical Design Applied to the MTBE and Methyl Acetate Reactive Distillation Column with Ternary Mixture," *AIChE J.*, **47**, 1333 (2001a).
Lee, J. W., S. Hauan, and A. W. Westerberg, "Feasibility of a Reactive Distillation Column with Ternary Mixtures," *Ind. Eng. Chem. Res.*, **40**, 2714 (2001b).
Lee, J. W., "Feasibility Studies on Quaternary Reactive Distillation Systems," *Ind. Eng. Chem. Res.*, **41**, 4632 (2002).
Levy, G. S., D. B. Van Dogen, and M. F. Doherty, "Design and Synthesis of Homogeneous Azeotropic Distillations. 2. Minimum Reflux Calculations for Non-ideal and Azeotropic Columns," *Ind. Eng. Chem. Fundam.*, **24**, 463 (1985).
Malone, M. F., and M. F. Doherty, "Reactive Distillation," *Ind. Eng. Chem. Res.*, **39**, 3953 (2000).
Mazzotti, M., B. Neri, D. Gelosa, A. Kruglov, and M. Morbidelli, "Kinetics of Liquid-Phase Esterification Catalyzed by Acidic Resins," *Ind. Eng. Chem. Res.*, **36**, 3 (1997).
Okasinski, M. J., and M. F. Doherty, "Design Method for Kinetically Controlled, Staged Reactive Distillation Columns," *Ind. Eng. Chem. Res.*, **37**, 2821 (1998).
Preston, K. L., "Use of Reactive Distillation in the Manufacture of Methyl Tert Butyl Ether," U.S. Patent No. 5,741,953 (1998).
Seydel, R., and V. Hlaváček, "Role of Continuation in Engineering Analysis," *Chem. Eng. Sci.*, **42**, 1281 (1987).
Smith, L. A., "Catalytic Distillation Process," U.S. Patent No. 4,307,254 (1981).
Smith, L. A., "Process for the Preparation of MTBE," U.S. Patent No. 5,118,873 (1992).
Stankiewicz, A. I., and J. A. Moulijn, "Process Intensification: Transforming Chemical Engineering," *Chem. Eng. Prog.*, **96**(1), 22 (2000).
Stichlmair, J. G., and J. R. Fair, *Distillation: Principle and Practice*, Wiley, New York (1998).
Taylor, R., and R. Krishna, "Modelling Reactive Distillation," *Chem. Eng. Sci.*, **55**, 5183 (2000).
Venimadhavan, G., G. Buzad, and M. F. Doherty, "Effects of Kinetics on Residue Curve Maps for Reactive Distillation," *AIChE J.*, **40**, 1814 (1994).
Venkataraman, S., W. K. Chan, and J. F. Boston, "Reactive Distillation Using Aspen Plus," Chem. Eng. Prog., **86**(8), 45 (1990).
Watzdorf, v., J. Bausa, and W. Marquardt, "Shortcut Method for Non-ideal Multicomponent Distillation: 2. Complex Columns," *AIChE J.*, **45**, 1615 (1999).
Xu, Z. P., and K. T. Chuang, "Kinetics of Acetic Acid Esterification over Ion Exchange Catalysts," *Can. J. Chem. Eng.*, **74**, 493 (1996).

Appendix A: Material and Heat Balance Equations

Here, we assume that all reaction molar holdups (or *Da*'s) for each stage are equal (Buzad and Doherty, 1994).

Reactive Stripping Section Around the Balance Envelope in Figure 6. The material balance equation becomes

$$L_n \boldsymbol{x}_n = V_{n+1}\boldsymbol{y}_{n+1} + B\boldsymbol{x}_B - \nu H \sum_{i=B}^{n+1} r_i \qquad \text{(A1)}$$

where H is the molar holdup, r_i is the reaction rate on stage i, and $\boldsymbol{\nu}$ is the stoichiometric vector. Index $i = B$ represents the bottom stage.

The reaction rate is generally expressed by mole fractions for isomolar reactions and activities for nonisomolar reactions. For the derivation purpose, let's consider the kinetics based on activity because the mole-based kinetics is one of special cases for the activity coefficients equal to one

$$r_i = k_{f,i}\left(\prod_{k=1}^{NP} a_{k,i}^{|\nu_k|} - K_{eq}\prod_{l=1}^{NR} a_{l,i}^{|\nu_l|}\right) \qquad \text{(A2)}$$

where $k_{f,i}$ is the forward reaction constant at stage i (function of stage temperature), $a_{k,i}$ is the activity of product k at stage i, $a_{l,i}$ is the activity of reactant l at stage i, K_{eq} is the reaction equilibrium constant, NP is the number of products, NR is the number of reactants, ν_k is the reaction coefficient for reactant k, and ν_l is the reaction coefficient for product l.

If we insert Eq. A2 into Eq. A1 and introduce $Da = (Hk_{f,\text{ref}})/F$, Eq. A1 becomes

$$L_n \boldsymbol{x}_n = V_{n+1}\boldsymbol{y}_{n+1} + B\boldsymbol{x}_B - \boldsymbol{\nu} FDa \sum_{i=B}^{n+1} \frac{k_{f,i}}{k_{f,\text{ref}}}\left(\prod_{k=1}^{NP} a_{k,i}^{|\nu_k|} - K_{eq}\prod_{l=1}^{NR} a_{l,i}^{|\nu_l|}\right) \qquad \text{(A3)}$$

where $k_{f,\text{ref}}$ is the forward reaction constant evaluated at the reference temperature.

Since all enthalpy data are based on the elemental reference condition, they include the heat of reaction (Venkataraman et al., 1990) implicitly. So, the heat balance equation around the balance envelope in Figure 6 yields

$$L_n h_n = V_{n+1}H_{n+1} + B(h_B - q_B) \qquad \text{(A4)}$$

where h_n is the liquid molar enthalpy at stage n, H_{n+1} is the vapor molar enthalpy at stage $n+1$, h_B is the bottom product molar enthalpy, and q_B is the reboiler molar duty.

Reactive Rectifying Section. In the same way as for the stripping section, the material and heat balance equations are

$$V_{m+1}\boldsymbol{y}_{m+1} = L_m\boldsymbol{x}_m + D\boldsymbol{x}_D - \boldsymbol{\nu}FDa\sum_{i=1}^{m}\frac{k_{f,i}}{k_{f,\mathrm{ref}}}\left(\prod_{k=1}^{NP}a_{k,i}^{|\nu_k|} - K_{eq}\prod_{l=1}^{NR}a_{l,i}^{|\nu_l|}\right) \quad \text{(A5)}$$

$$V_{m+1}H_{m+1} = L_m h_m + D(h_D - q_D) \quad \text{(A6)}$$

where h_D is the distillate molar enthalpy, and q_D is the condenser molar duty. Index $i=1$ represents the top stage.

Appendix B: Determination of a Damköhler Number

Up to stage $n+1$ in Figure 6, Eq. A1 can be rearranged to

$$L_{n+1}\boldsymbol{x}_{n+1} = V_{n+2}\boldsymbol{y}_{n+2} + B\boldsymbol{x}_B - \boldsymbol{\nu}F\frac{Da}{k_{f,\mathrm{ref}}}\sum_{i=B}^{n+2}r_i = V_{n+2}\boldsymbol{y}_{n+2} + B\boldsymbol{x}_B - \boldsymbol{\nu}\xi_{n+2} \quad \text{(B1)}$$

Thus, if we compare the reaction terms only, ξ_{n+2} becomes

$$\xi_{n+2} = F\frac{Da}{k_{f,\mathrm{ref}}}\sum_{i=B}^{n+2}r_i \quad \text{(B2)}$$

If we add one more stage (stage $n+1$), ξ_{n+1} becomes

$$\xi_{n+1} = F\frac{Da}{k_{f,\mathrm{ref}}}\sum_{i=B}^{n+1}r_i \quad \text{(B3)}$$

Taking the difference, $(\xi_{n+1} - \xi_{n+2})$, Da is calculated by the following equation

$$Da = \frac{\xi_{n+1} - \xi_{n+2}}{(F/k_{f,\mathrm{ref}}) * r_{n+1}} \quad (B4)$$

Manuscript received May 21, 2002, and revision received Dec. 10, 2002.

In the same way, we can also obtain Da for the reactive rectifying section

$$Da = \frac{\xi_{m+1} - \xi_m}{(F/k_{f,\mathrm{ref}}) * r_{m+1}} \quad \text{(B5)}$$

Reaction kinetics for three reactive systems

2-pentene decomposition into 2-butene and 3-hexene (Okasinski and Doherty, 1998)

Reaction: $2C_5^{=} \leftrightarrow C_4^{=} + C_6^{=}$

Reaction rate: $r_{C6} = k_f\left(\boldsymbol{x}_{C5}^2 - \boldsymbol{x}_{C5}\boldsymbol{x}_{C6}/K_{eq}\right)$

$k_f = 29.6133\exp(-3321.24/T)\ \mathrm{s}^{-1}$, T: Kelvin

$K_{eq} = 0.25$

$k_{f,\mathrm{ref}}$ at 298.15 K

Methyl acetate production system (Xu and Chuang, 1996; Mazzotti et al., 1997)

Reaction: $AC + MT \leftrightarrow MA + W$

Reaction rate: $r_{MA} = k_f\left(\boldsymbol{x}_{AC}\boldsymbol{x}_{MT} - \boldsymbol{x}_{MA}\boldsymbol{x}_W/K_{eq}\right)$

$k_f = 1.76 * 10^7\exp(-7032.1/T)\ \mathrm{s}^{-1}$, T: Kelvin

$K_{eq} = 5.2$

$k_{f,\mathrm{ref}}$ at 332.20 K

MTBE production system (Venimadhavan et al., 1994)

Reaction: $IC_4^{=} + MT \leftrightarrow MTBE$

Reaction rate: $r_{MTBE} = k_f\left(a_{C4}a_{MT} - a_{MTBE}/K_{eq}\right)$

$k_f = 1.24\exp(-3187/T)\ \mathrm{s}^{-1}$, T: Kelvin

$K_{eq} = -16.33 + 6820.0/T$, T: Kelvin

$k_{f,\mathrm{ref}}$ at 410.05 K